General Disclaimer

One or more of the Following Statements may affect this Document

- This document has been reproduced from the best copy furnished by the organizational source. It is being released in the interest of making available as much information as possible.

- This document may contain data, which exceeds the sheet parameters. It was furnished in this condition by the organizational source and is the best copy available.

- This document may contain tone-on-tone or color graphs, charts and/or pictures, which have been reproduced in black and white.

- This document is paginated as submitted by the original source.

- Portions of this document are not fully legible due to the historical nature of some of the material. However, it is the best reproduction available from the original submission.

FEASIBILITY STUDY OF VELOCITY SYNCHRONIZED FOURIER TRANSFORM HOLOGRAM CAMERA SYSTEM

By John H. Ward, William A. Dyes, and Bruce J. McCabe

April 1969

Report No. TO-B 69-24

Prepared under Contract No. NAS 12-2030
TECHNICAL OPERATIONS, INCORPORATED
Burlington, Massachusetts

Electronics Research Center

NATIONAL AERONAUTICS AND SPACE ADMINISTRATION

Mr. Earl Klaubert
Technical Monitor
NAS 12-2030
Electronics Research Center
575 Technology Square
Cambridge, Massachusetts 02139

Requests for copies of this report should be referred to:

NASA Scientific and Technical Information Facility
P. O. Box 33, College Park, Maryland 20740

FEASIBILITY STUDY OF VELOCITY SYNCHRONIZED FOURIER TRANSFORM HOLOGRAM CAMERA SYSTEM

By John H. Ward, William A. Dyes, and Bruce J. McCabe

April 1969

Report No. TO-B 69-24

Prepared under Contract No. NAS 12-2030
TECHNICAL OPERATIONS, INCORPORATED
Burlington, Massachusetts

Electronics Research Center

NATIONAL AERONAUTICS AND SPACE ADMINISTRATION

TABLE OF CONTENTS

LIST OF ILLUSTRATIONS

LIST OF ILLUSTRATIONS (Concluded)

LIST OF TABLES

DESIGN OF VELOCITY SYNCHRONIZED FOURIER TRANSFORM HOLOGRAM CAMERA SYSTEM

By John H. Ward, William A. Dyes, and Bruce J. McCabe

Technical Operations, Incorporated
Burlington, Massachusetts

SECTION 1

SUMMARY

Methods for recording holograms of hypervelocity particles were studied in this program. It was assumed that the particle would move an appreciable distance during the hologram exposure time. The problem was to find a method of maintaining stationary hologram interference fringes as the object traveled across the field of view. A Fourier transform method employing an interferometer and using a reference beam produced by back reflection from the object was found to be conceptually correct. The stationarity of this approach was demonstrated experimentally.

Several experiments were carried out to determine the feasibility of building a hologram system to record hypervelocity particles based on the Fourier transform method. The stationarity of standard lenses was investigated and found to be sufficient. The brightness and uniformity of the back reflected reference beam was measured and found to be marginal. The resolution of Fourier transform holograms of opaque objects on a bright background was tested and found to be limited to 10 to 15 line/mm.

SECTION 2

INTRODUCTION

The purpose of this contract was to design a hologram system to be used to record particles in the size range of 50 to 100 μ diameter moving at velocities of 0 to 50 Km/sec. Conventional hologram systems would have difficulty in stopping the motion of the particles at these velocities, (Ref. 1). At 20 Km/sec a particle would move 100μ during a 5×10^{-9} sec Q-switched laser pulse. The reconstructed image from such a hologram would at best be a smear having a width corresponding to the diameter of the particle. Good resolution of moving particles can be obtained when the particle moves at most one fifth of its diameter during the laser pulse time. This would set an upper limit for a 50μ particle at about 2 Km/sec with a 5×10^{-9} sec pulse duration. An additional problem would be met in trying to synchronize the arrival of the particle with such a short pulse.

Conventional incoherent imaging systems have the same basic problems of stopping the object motion and of synchronization. Incoherent systems also pose an additional problem because of the very limited depth of field. To obtain good resolution of a 50μ particle an f/20 imaging system is needed with incoherent light. The focal tolerance of the system would be approximately ± 0.1 mm (Ref. 2).

Under this contract, Fourier transform holograms (Ref. 3) were studied to develop a camera system which would have automatic velocity synchronization as well as good depth of field and resolution.

The approach taken was based on two assumptions. The first assumption was that the diffraction pattern of an object traveling perpendicular to the optical axis in the front focal plane of a lens is stationary in space when observed in the back focal plane of the same lens. The second assumption was that a coherent reference beam could be derived by reflection from the particle and could be used to form a hologram of the object in the back focal plane of the lens. Under this study both theoretical and experimental analyses of implementing such a hologram system have been carried out. It is concluded that although such a system is conceptually feasible, it would be difficult to fabricate. The major weakness of such an approach is the lack of spatial resolution currently obtained in Fourier transform holograms. This difficulty is covered in the experimental discussion.

SECTION 3

THEORETICAL BACKGROUND

This section is a theoretical outline of Fourier transform holograms and a summary of the various requirements of the system under investigation. Particular calculations and derivations used for analysis of the experimental data are included in the following subsection.

3.1 Fourier Transforms Using a Lens

Figure 1 is a schematic of a Fourier transform optical system. A coherent collimated light beam is incident on the object plane from the left. The object plane is located a distance Δ beyond the front focal plane. The amplitude distribution in the back focal plane of the lens will be the Fourier transform of the object amplitude distribution. When the Fourier transform is observed or recorded on photographic film, the intensity is proportional to the square magnitude of the Fourier transform. The intensity distribution seen in the back focal plane is the Fraunhofer diffraction pattern of the object.

Using the Green function method outlined by Beran and Parrent (Ref. 4) the expression for the amplitude in the back focal plane of the lens is

$$A(\vec{y}) = -\frac{k^2}{4\pi^2} \int\int O(\vec{x}) \frac{e^{ikr}}{r} \frac{e^{ikr'}}{r'} e^{-\frac{ik|\vec{\rho}|^2}{2f}} d\vec{x}\, d\vec{\rho} \,. \qquad (1)$$

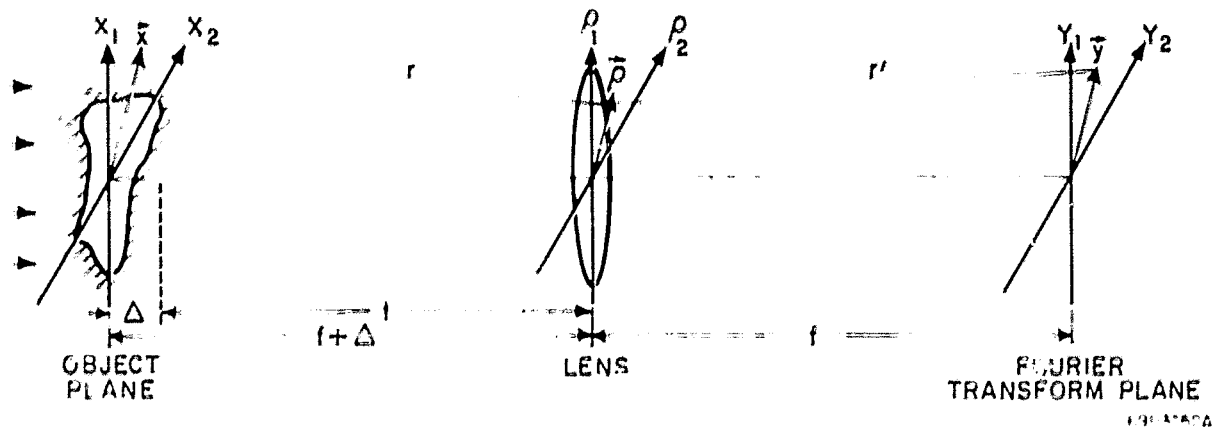

Figure 1. Schematic of a Fourier Transform Optical System

Here, k is the wave number $2\pi/\lambda$ and $O(\vec{x})$ is the amplitude of the light over the object. Distances r and r′ are defined from Figure 1 as

$$r = \left| f^2 + \left| \vec{x} - \vec{\rho} \right|^2 \right|^{1/2} \tag{2}$$

$$r' = \left| f^2 + \left| \vec{y} - \vec{\rho} \right|^2 \right|^{1/2} .$$

The double integration is carried out over the object plane and over the aperture of the lens. The distances r and r′ can be approximated as

$$r \simeq f + \Delta + \frac{|\vec{x}|^2}{2(f+\Delta)} + \frac{|\vec{\rho}|^2}{2(f+\Delta)} - \frac{\vec{x}\cdot\vec{\rho}}{(f+\Delta)} + \cdots$$

$$r' \simeq f + \frac{|\vec{\rho}|^2}{2f} + \frac{|\vec{y}|^2}{2f} - \frac{\vec{y}\cdot\vec{\rho}}{f} + \cdots \tag{3}$$

Keeping only first order terms in the denominator and second order terms in the exponentials in Equation (1) gives

$$A(\vec{y}) = \frac{k^2}{4\pi^2 f(f+\Delta)} e^{ik(2f+\Delta)} \int\int O(\vec{x}) \exp^{ik} \left(\frac{|\vec{x}|^2}{2(f+\Delta)} + \frac{|\vec{\rho}|^2}{2(f+\Delta)} \right.$$

$$\left. + \frac{|\vec{y}|^2}{2f} - \frac{\vec{\rho}\cdot\vec{y}}{f} - \frac{\vec{\rho}\cdot\vec{x}}{(f+\Delta)} \right) d\vec{\rho}\, d\vec{x} . \tag{4}$$

Completing the square of the exponential terms gives

$$A(\vec{y}) = C\, e^{ik\Delta}\, e^{-\frac{ik|\vec{y}|^2\Delta}{2f^2}} \int O(\vec{x})\, e^{-\frac{ik\vec{x}\cdot\vec{y}}{f}} \left[\int \exp ik \left(\frac{\vec{\rho}}{\sqrt{2(f+\Delta)}} - \frac{\vec{x}}{\sqrt{2(f+\Delta)}} - y\sqrt{\frac{(f+\Delta)}{2f^2}}\right) d\vec{\rho}\right] d\vec{x} \quad . \tag{5}$$

If the lens aperture radius, a, meets the condition

$$a^2 >> \frac{2(f+\Delta)}{k} \quad , \tag{6}$$

then the integration over the ρ plane, the lens aperture, yields a constant. In this case the expression for the amplitude at the back focal plane becomes (Ref. 3)

$$A(\vec{y}) = C'\, e^{ik\Delta}\, e^{-\frac{ik|\vec{y}|^2\Delta}{2f^2}} \int O(\vec{x})\, e^{-\frac{ik\vec{x}\cdot\vec{y}}{f}}\, d\vec{x} \quad . \tag{7}$$

Thus, we have the spatial Fourier transform of the object amplitude distribution multiplied by two phase factors which are dependent upon Δ, the distance of the object beyond the front focal plane of the lens. All other factors have been absorbed into the constant C'. The quadratic phase factor in the back focal plane results because the wave front is spherical if Δ is not zero. This leads to a diverging wave front if Δ is negative and the object is located between the front focal plane and the lens; a converging wave front is produced if the object lies beyond the front focal plane and Δ is positive.

Equation (7) can be written more compactly as

$$A(\vec{y}) = C'\, e^{ik\Delta}\, e^{-\frac{ik|\vec{y}|^2\Delta}{2f^2}}\, \tilde{O}\left(\frac{\vec{y}k}{f}\right) \quad . \tag{8}$$

$\tilde{O}(\vec{y}k/f)$ is the Fourier transform of the object with an argument in dimensions of spatial frequency, radians per unit length.

Two useful results can be proven from Equation (7). First, if the object is translated an amount $\vec{x}_o$ in the object plane, Equation (8) becomes

$$A(\vec{y}) = C' e^{ik\Delta} e^{-\frac{ik|\vec{y}|^2\Delta}{2f^2}} e^{\frac{ik\vec{x}_o\cdot\vec{y}}{}} \tilde{O}\left(\frac{\vec{y}k}{f}\right) . \tag{9}$$

Thus, the Fourier transform of the object remains centered on the optical axis, but it is now multiplied by a linear phase $k\vec{x}_o \cdot \vec{y}/f$. The light distribution arrives at the transform plane from an off-axis direction. The angle α between the optical axis of the lens and the direction of arrival is determined by

$$\sin\alpha = \frac{|\vec{x}_o|}{f} . \tag{10}$$

It can be shown by taking the square magnitude of the amplitudes in Equations (8) and (9) that the intensity of the light in the transform plane does not change as the object is translated.

Conversely, if the object is illuminated by a collimated beam at an angle α to the optical axis, it follows from Equation (7) that the Fourier transform is displaced. Equation (8) becomes

$$A(\vec{y}) = C' e^{ik\Delta} e^{-\frac{ik|\vec{y}+\vec{y}_o|^2\Delta}{f^2}} \tilde{O}\left(\frac{(\vec{y}+\vec{y}_o)k}{f}\right) \tag{11}$$

where $|\vec{y}_o| = f \sin\alpha$.

Thus, the center of the diffraction pattern Fourier transform lies off the optical axis by the distance $|\vec{y}_o|$ determined by the angle α from Equation (11). However, since the object was not translated the light still arrives at the back focal plane along the optical axis. This fact must be considered when designing the particle hologram camera.

3.2 Fourier Transform Holograms

To produce a Fourier transform hologram a coherent plane wave reference beam must be added at an angle to the object Fourier transform described in Equation (7). The interference pattern formed between the reference beam and the object transform

is recorded on film and becomes the hologram (Ref. 3). The intensity in the transform plane can be written as

$$|A(\vec{y})|^2 = \left| e^{iky_1 \sin\Theta} + C' e^{ik\Delta} e^{-\frac{ik|\vec{y}|^2\Delta}{2f^2}} e^{ik\vec{x}_o \cdot \vec{y}} \tilde{O}\left(\frac{\vec{y}k}{f}\right) \right|^2 . \qquad (12)$$

Here, a plane wave of unit amplitude is added coherently at the direction Θ in the plane formed by the optical axis and y_1 axis as drawn in Figure 2. Equation (9) has been used to represent the object Fourier transform. Equation (12) can be written as

$$|A(\vec{y})|^2 = \left(1 + 2\,\mathrm{Re}\left[C' e^{ik\left(\Delta - y_1 \sin\Theta + \frac{\vec{x}_o \cdot \vec{y}}{f} - \frac{|\vec{y}|^2\Delta}{2f^2}\right)} \tilde{O}\left(\frac{k\vec{y}}{f}\right)\right] + |C'|^2 \left|\tilde{O}\left(\frac{k\vec{y}}{f}\right)\right|^2\right) . \qquad (13)$$

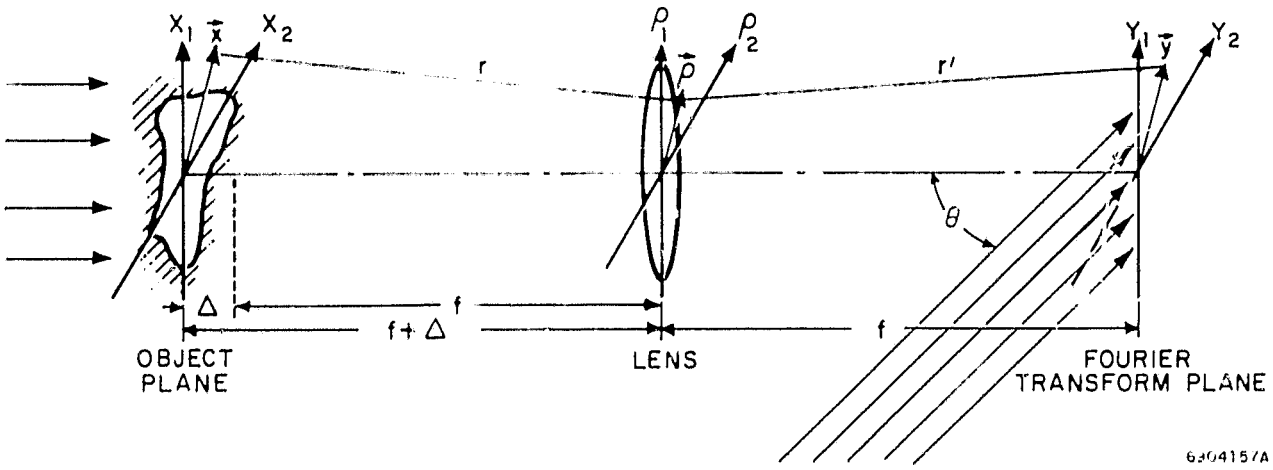

Figure 2. Schematic of Fourier Transform Hologram Optical System

In Equation (13) the first term is the intensity of the plane wave reference beam and the last term is the diffraction pattern of the object. The second term is due to the interference of the two beams and is the hologram. It is an interference fringe pattern, the exponential term, modulated by the amplitude of the object diffraction pattern. In order to describe the properties of the interference pattern due to the several exponential terms, we consider the object to be a point source of light. In this case the Fourier transform of the object becomes a plane wave. If the object

point source is located at the front focal point of the lens ($\Delta = 0$, $\vec{x}_o = 0$) the interference fringes are linear and parallel to the y_2 axis at a spatial frequency of k sin Θ radians per millimeter. Also, in this case there will be an intensity maximum on axis at $|\vec{y}| = 0$.

If the point object remains on axis ($\vec{x}_o = 0$) but is moved along the optical axis by a distance Δ, two more terms in the exponential come into play. On axis in the transform plane ($\vec{y} = 0$) the center fringe goes through its maximum and minimum values as the point object is moved through units of λ, the optical wave length. Off axis the fringes are no longer linear, but are curved and have an increasing frequency by the amount $k|\vec{y}|\Delta/2f^2$. This is because a spherical wave front from the point object is now interfering with a plane wave reference beam. The effects of the quadratic term are far less pronounced, since for most conditions

$$\frac{|\vec{y}|_{max}}{2f^2} << 1. \tag{14}$$

If the point object is placed off axis at $\vec{x}_o$ in the front focal plane ($\Delta = 0$), the interference fringes now change direction and frequency but remain linear. The new spatial frequency is

$$\omega = k\left(\frac{x_2^2 + x_1^2}{f^2} + \sin^2\Theta - \frac{x_1 \sin\Theta}{f}\right)^{1/2} \text{ radians/mm.} \tag{15}$$

Here x_1 and x_2 are the components of $\vec{x}_o$ along the x_1 and x_2 axes in the object plane. The fringe direction in the transform plane is no longer parallel with the y_2 axis but stands at an angle ϕ to the y_2 axis, where ϕ is given by

$$\sin\phi = \frac{kx_2}{f\omega} \quad . \tag{16}$$

Thus, it is apparent that although the diffraction pattern intensity is not a function of Δ or $\vec{x}_o$ in the Fourier transform plane, its phase is. This phase is the result of the object diffracted light arriving at the transform plane from a different direction depending on position $\vec{x}_o$ or arriving as a diverging or converging spherical wave depending upon the displacement Δ.

These interference fringes caused by the position of the object ($\vec{x}_o, \Delta$) will cause the reconstructed image to fall at the proper place in the field of view when the hologram is reconstructed. If the object is translated, the interference fringes formed using a fixed reference beam also move. The light level at any fixed spatial point in the transform plane will go through maximum and minimum intensity values as the object moves. The contrast, visibility, of the interference fringes can be computed from Equation (13) and is proportional to the second term of the equation.

The second term of Equation (13) would vanish during a time exposure which integrated, averaged, over a few cycles of intensity variation from maximum to minimum values. The resulting fringe visibility would be zero. This corresponds to allowing the object to move a few wavelengths in any direction during the exposure. A motion of even 1/5 wavelength is usually sufficient to reduce contrast to the point of degrading the reconstructed image.

Thus, in order to form a Fourier transform hologram of a moving object, interference fringes which depend on the object position through $\vec{x}_0$ and Δ must be eliminated. This, of course, removes all information as to the object's position in the field of view when the hologram was made. All objects hologrammed in such a system would reconstruct at the same position. In order to eliminate object position dependent fringes, any motion of the object has to be instantaneously compensated for by a corresponding change in direction of the reference beam. This can be done by deriving a reference beam by reflection from the object.

One such system was found and investigated although undoubtedly a whole class of similar systems can be conceived. However, no system can be found which will correct for rotation of an arbitrarily shaped object.

3.3 Reconstruction of Fourier Transform Holograms

This subsection briefly describes the reconstruction of Fourier transform holograms of stationary objects. For a more complete description, the reader should refer to the work of DeVelis and Reynolds (Ref. 3) or Stroke (Ref. 5).

First, it is assumed that the intensity given by Equation (13) is recorded properly such that the amplitude transmission of hologram is proportional to the second term of Equation (13). The difficulties involved in this assumption will be very apparent in the following section covering the experimental results. It is this very difficulty which most limits the feasibility of building a Fourier transform hologram camera for small objects.

Since the hologram term in Equation (13) contains the Fourier transform of the object, a second optical Fourier transformation must be performed to reconstruct the image. The hologram is placed in the object plane of the optical system shown in Figure 2. The hologram term is made up of two terms which are complex conjugates of each other. Two images are reconstructed which lie at equal and opposite off-axis directions. The two images are mirror images of each other. The off-axis directions are determined by the phase terms linear in $\vec{y}$ (i.e., the interference fringe frequency as given by Equation (15)). If quadratic fringes are present in the hologram due to an object displacement Δ along the optical axis when recording the hologram, then one reconstructed image will focus a distance Δ in front of the back focal plane while its conjugate image will focus a distance Δ behind the back focal plane. This assumes that the same lens and optical wavelengths are used in both formation and reconstruction of the hologram. The first and third terms of Equation (13) contribute intensity at the center of the back focal plane during reconstruction.

It is important to note that if the forward diffracted beam from the object and the plane wave reference beam arrive at the hologram from the same direction, the linear fringes will be absent from the hologram in Equation (13). In this case both of the

the reconstructed images will focus on the optical axis and will not be separated from each other or from the contributions of the first and third terms. In this case the Fourier transform hologram is useless.

3.4 Fourier Transform Systems For a High Velocity Particle Camera

The feasibility of two different types of optical systems was investigated. In both systems (see Figures 3 and 4) a triangular arrangement of the beam splitters and a mirror was used to illuminate the object from two directions. The forward diffracted light was treated as the object beam which would produce the Fourier transform of the object cross sectional geometry in the back focal plane of a lens. The back reflected beam was considered to be the reference beam, since the back reflected light is in general more divergent than forward diffracted light. In the ideal case, the object would be a polished metal sphere which would produce a point source reference. Since the diffracted and reflected beams remain coherent with each other as the object is translated, the purpose of both optical systems (Figures 3 and 4) is to produce a fixed angle between the two beams while maintaining a spatially stationary interference pattern in a Fourier transform plane.

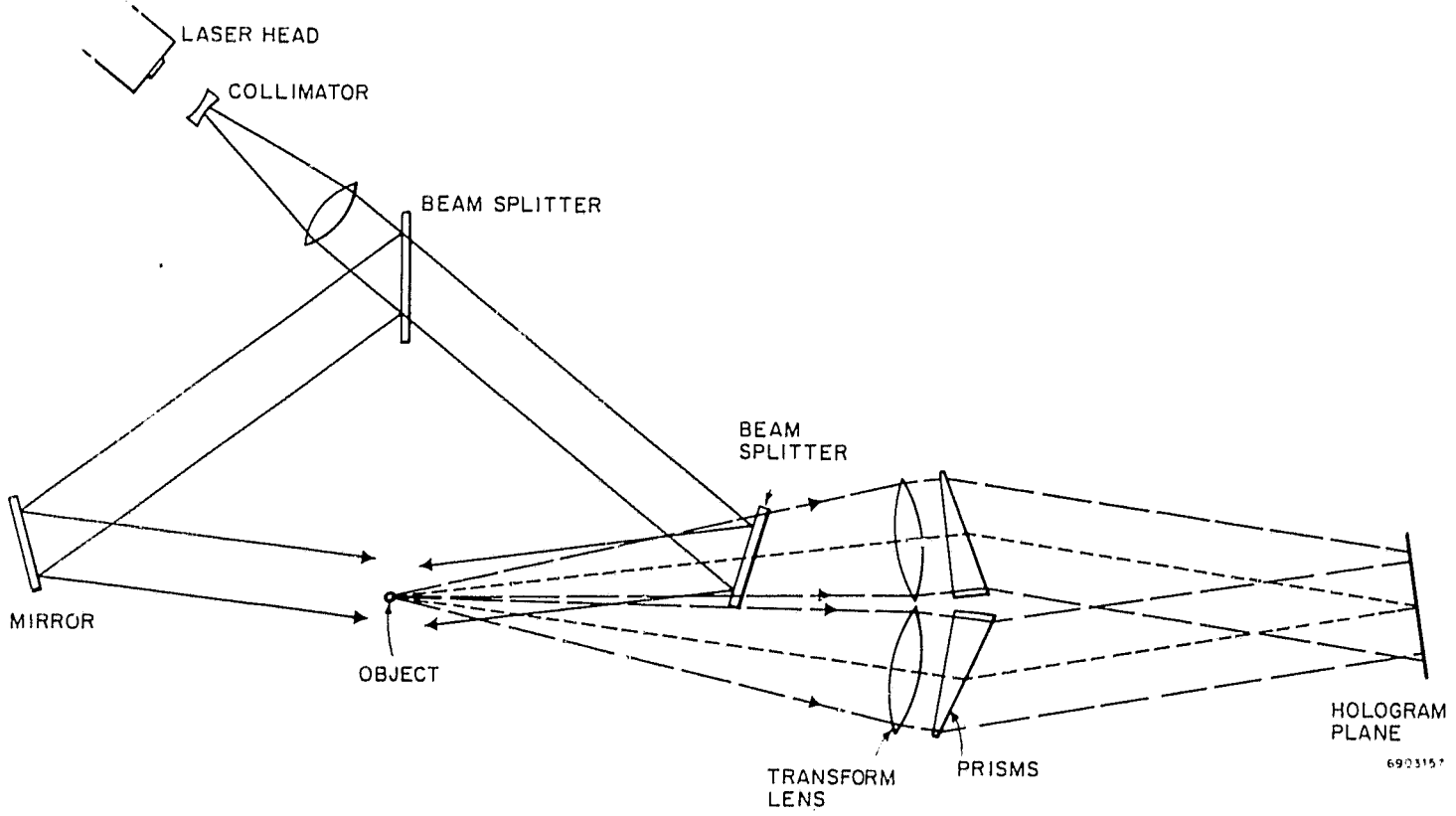

Figure 3. Possible Camera System with Coincident Front and Back Focal Points

Several other single lens systems were also considered during the course of this program. These were found unsatisfactory. It proved impossible to produce a spatially stationary fringe pattern while at the same time maintaining a fixed angle between the object and the reference beam as required by Equation (13).

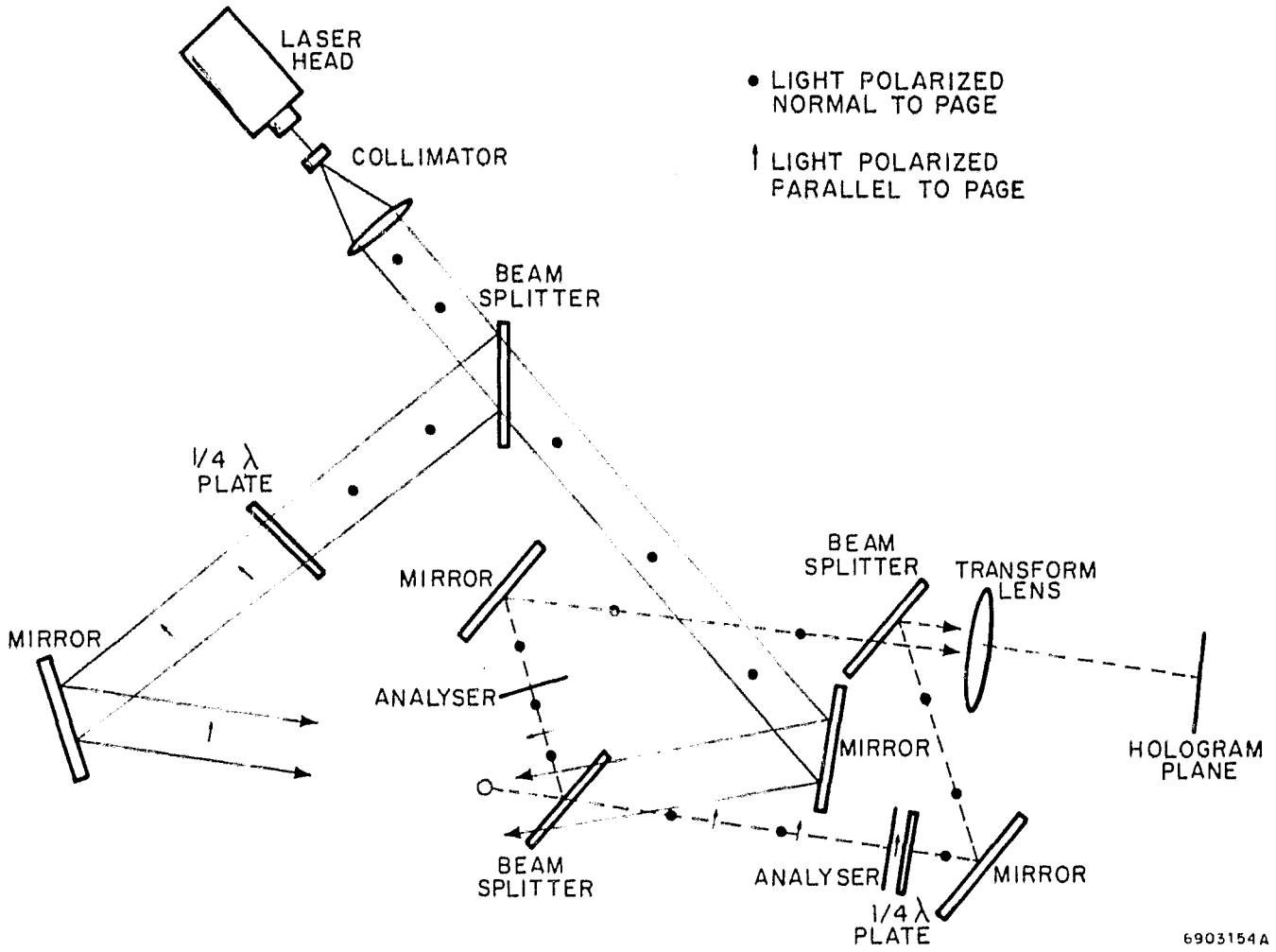

Figure 4. Possible Camera System with Coincident Back Focal Planes

3.4.1 System with Coincident Focal Points — In Figure 3 two symmetrical optical systems are arranged such that the front and back focal points are coincident and the optical axes are inclined at an angle. The object is assumed to be moving perpendicularly to the two axes and parallel to the line of intersection of the two front focal planes. The cone of forward-diffracted light is arranged to travel along the optical axis of the lower optical system. The back-reflected light will be collected primarily by the upper optical system.

From Equation (9), the amplitude of the forward diffracted light in the Fourier transform plane is

$$A(\vec{y}) = C\, e^{ik\Delta}\, e^{-\frac{ik|\vec{y}|^2\Delta}{2f^2}}\, e^{ik\vec{x}\cdot\vec{y}}\, \tilde{O}\left(\frac{\vec{y}k}{f}\right) \quad . \tag{17}$$

If the particle is assumed to be a sphere the amplitude of the back reflected light in the transform or hologram plane becomes by Equation (9)

$$A'(\vec{y}) = B\, e^{ik\Delta'}\, e^{-\frac{ik|\vec{y}|^2\Delta'}{2f}}\, e^{ik\vec{x}'\cdot\vec{y}}\, e^{ik \sin\Theta\, y_2} \quad . \tag{18}$$

The prime and unprime coordinates in Equations (17) and (18) refer to the object's position relative to the front focal planes of the upper and lower optical systems respectively. The instantaneous intensity in the hologram plane is

$$|A(y) + A'(y)|^2 = |B|^2 + \left| C\, \tilde{O}\, \frac{\vec{y}k}{f} \right|^2$$

$$+ 2\,\mathrm{Re}\left\{ C\, B^*\, e^{ik(\Delta - \Delta')}\, e^{ik\vec{y}\cdot(\vec{x}-\vec{x}')} \right. \tag{19}$$

$$\left. e^{-\frac{ik|\vec{y}|^2}{2f^2}(\Delta - \Delta')}\, e^{ik \sin\Theta\, y_2}\, \tilde{O}\left(\frac{\vec{y}k}{2f}\right) \right\} \quad .$$

Here, Θ is the angle between the two optical axes at the hologram plane. In Equation (19) the third term is the hologram term and the first two terms are the intensities due to the two beams separately. In the hologram the exponential phase factor with argument $k \sin\Theta\, y_2$ produces linear interference fringes of fixed frequency which will cause the two images to reconstruct off axis in equal and opposite directions. The phase factor in $k(\Delta - \Delta')$ determines if a fringe maximum or minimum falls on axis. The quadratic phase factor will again cause the reconstructed images to focus displaced by $\pm\ (\Delta - \Delta')$ from the back focal plane of the reconstructing lens. The quantity $\vec{y}\cdot(\vec{x} - \vec{x}')$ produces an additional linear phase factor.

We now choose the x_1 and x'_1 directions in the two front focal planes to run parallel to the line of intersection of the two planes. This implies that the x_2 and x'_2 directions are inclined to each other at the same angle, α, as the optical axes. As long as the motion of the object remains parallel to the x_1 and x'_1 direction the quantities $(\Delta - \Delta')$ and $\vec{y}\cdot(\vec{x} - \vec{x}')$ are constant. In this case the interference fringes as spatially stationary and a hologram may be recorded even though the particle moves during the laser pulse time. However if the particle does not travel parallel to x_1 and x'_2, the quantities $(\Delta - \Delta')$ and $\vec{y}\cdot(\vec{x} - \vec{x}')$ are not constant in time and the fringes move. Suppose, for example, the particle remains in the front focal plane of the lower optical system but has a velocity component v_2 along the x_2 direction. The quantity $(\Delta - \Delta')$ now has a time varying component $v_2 \sin\alpha$. The most that $(\Delta - \Delta')$ can be allowed to change during the exposure time is on the order of $\lambda/2$. With a total motion of 2 mm during the laser pulse and a value of $\sin\alpha$ of 0.2, the particle direction must lie parallel to x_1 and x'_1 to within 10^{-3} radians.

Thus, the system shown in Figure 3 gives a stationary hologram only for one exact translation direction. For translation of the particle in other directions, it is only approximately stationary depending upon the direction, speed, and laser pulse time. Similar effects would occur in any optical configuration in which the focal planes of the object and reference beams were inclined at an angle. Since these systems are only approximately stationary, they were not investigated experimentally.

3.4.2 System with Coincident Back Focal Planes – Figure 4 shows schematically a second optical system for making holograms of moving objects. Again a triangular arrangement is used to illuminate the particle from two directions. This time the laser beam must be linearly polarized. A 1/4 λ plate is introduced into one arm of the triangle to rotate the direction of polarization of the forward diffracted beam by 90 degrees. A modified Mach-Zehnder interferometer is placed between the particle and transform lens. The optical axes of the two arms of the interferometer are displaced by moving the last beam splitter slightly out of its usual position. However, the interferometer is set up to keep the two axes parallel. The analyzer in the upper arm of the interferometer is aligned to pass only the plane polarized back-reflected light. This light again serves as a coherent reference beam. The analyzer in the lower arm is aligned to pass only the forward-diffracted light. A 1/4 λ plate is then used to rotate the plane of polarization back to that of the reference beam so that interference can take place. Both beams then enter the transform plane. The parallel displacement introduced by the interferometer between the two beams produces linear interference fringes in the back focal plane. This becomes more apparent by consideration of Equation (9). A mathematical analysis of this system would give a result for the hologram intensity similar in form to Equation (19) derived for the previous system. However, in this system, since the beams enter the lens parallel, the front focal planes are parallel although they may be displaced along the optical axis due to unequal path lengths. Since the front focal planes are parallel, the intensity in the hologram plane will remain stationary independent of the direction of translation and no tolerance need be given on particle flight direction. This system was investigated experimentally.

SECTION 4

EXPERIMENTAL RESULTS

This section describes the several experiments which were carried out to establish the feasibility of building a system to record high speed particles.

4.1 Fringe Stationarity

Tests were first conducted to establish the experimental limits of the spatial stationarity of the Fourier transform intensity as the object is translated. The experimental setup is shown in Figure 5. Collimated laser light was allowed to fall on two 800μ pinholes separated by 5 mm. The interference fringe pattern was observed by a microscope and reticule focused in the transform plane. The pinholes were translated across the collimated beam while the fringe position was observed by the microscope. A fringe motion of one half fringe was used as a criterion to establish lack of stationarity. Table I gives the distance over which several lenses were determined to be stationary. This distance is symmetrically placed about the optical axis and represents a

region of stationarity. Any translation of the object within the circular region of stationarity did not change the position of the interference fringe pattern.

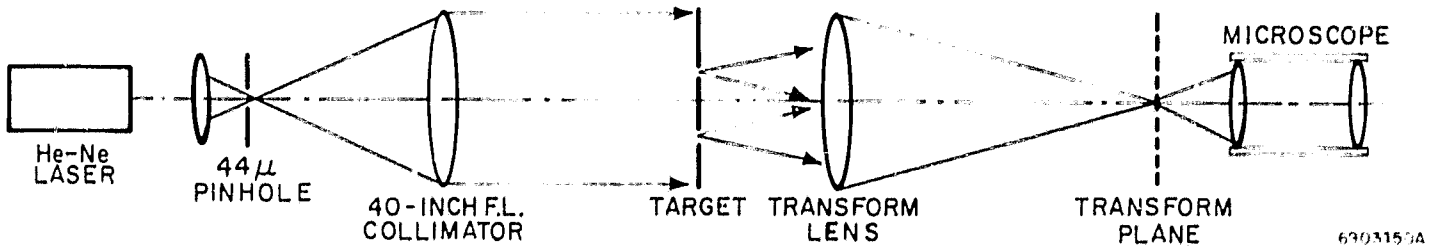

Figure 5. Experimental Setup to Check Transform Stationarity

TABLE I
LENS STATIONARITY DATA

Lens	Diameter Region of Stationarity (cm) Tolerance One Half Fringe Maximum Motion
15-inch Focal Length Jaeger Telescope Objective	2.0
4-inch Focal Length Jaeger Achromate	1.4
135-mm Focal Length Enlarging Lens	3.0
75-mm Focal Length Schneider Xenon	0.3

Figure 6 demonstrates the reduction of contrast as the two pinholes are translated to the point of losing stationarity. These pictures were recorded using the 15-inch focal length Jaeger telescope objective. A translation of 1 cm was used in Figure 6(a). Here, the fringes had not moved as a double exposure was made. In Figure 6(b), a translation of 2 cm was used between exposures and the lack of stationarity is evident from the reduction of contrast.

As a further check on the effects of lack of stationary, holograms were recorded using the 15-inch Jaeger lens. The setup is shown in Figure 7. A 3.5X microscope lens was mounted baside the target on the translating stage to provide a point reference source. The target, object, is shown in Figure 8. Holograms were recorded on AHU microfile film and developed to a gamma of 1 in Microdol-X for 5 minutes at 68°F. Figure 9 shows the diffraction pattern of the target "3"; Figure 10 shows the hologram of the stationary "3".

Linear fringes due to the interference between the object diffracted light and the reference beam are apparent over most of the area shown in Figure 10. The lowest exposure in Figure 10 is determined by the reference beam. This lowest level is centered on the linear part of the D vs. log E curve of the film. Thus regions of

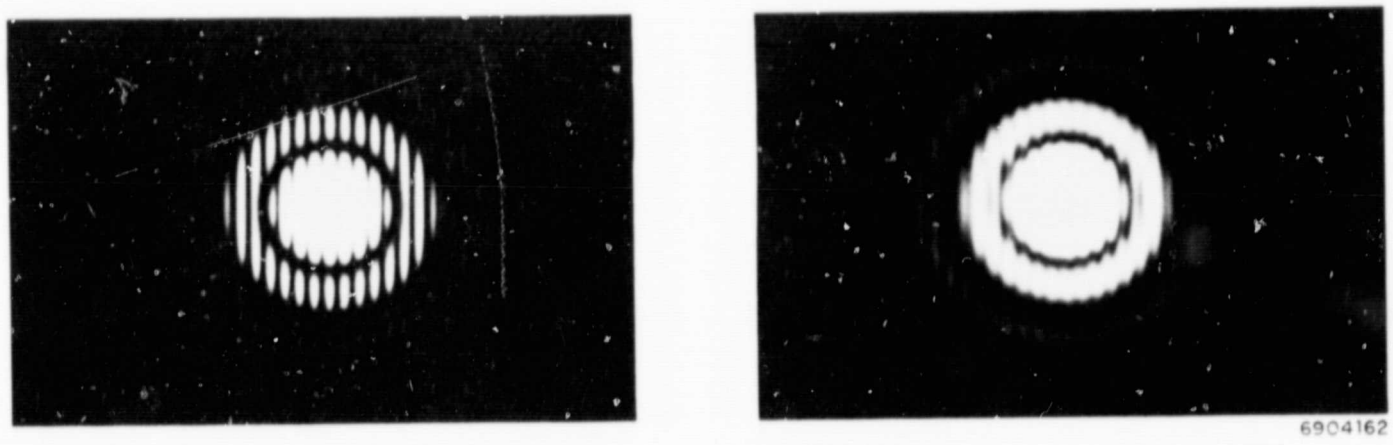

6904162

(a) 1 cm Translation Between Exposures (b) 2 cm Translation Between Exposures

Figure 6. Results of the 2-Pinhole Test for Fringe Stationarity

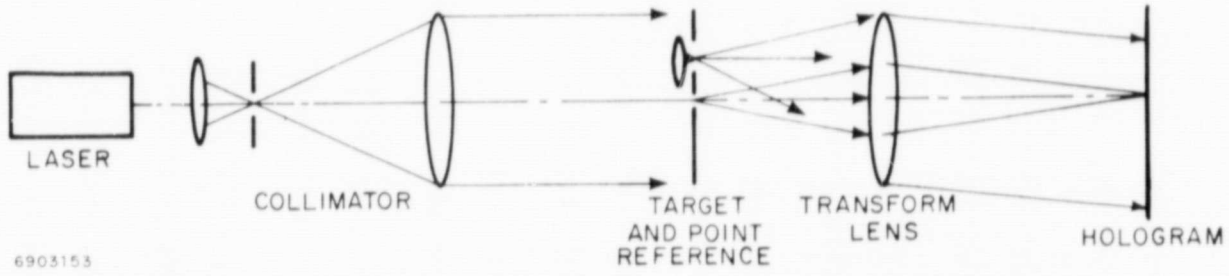

Figure 7. Setup for Making Fourier Transform Holograms with a Synchronized Reference Beam

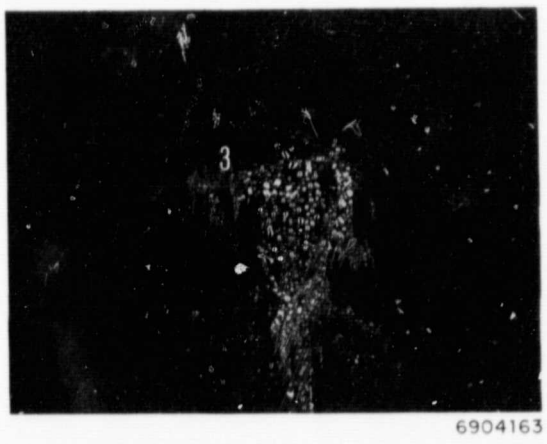

Figure 8. Target of Transparent "3" on a Dark Background. (The line width of the "3" is approximately 110 μ. The magnification in the print is 15X.)

Figures 9 and 10 of low exposure are enhanced by the addition of the reference beam. Without the reference beam these regions fall down on the toe of the D vs. log E curve. Figure 11 is the reconstructed image from the hologram shown in Figure 10.

As a further check of stationarity, holograms were made by using three exposures with the object being translated between exposures. Figure 12 shows the reconstructed images for different amounts of translation. The holograms reconstruct quite well until Figure 12(d) which had an object translation of 2.4 cm. The result corresponds well with the results of the 2-pinhole test of the 15-inch focal length Jaeger lens.

(a) At 40X Enlargement

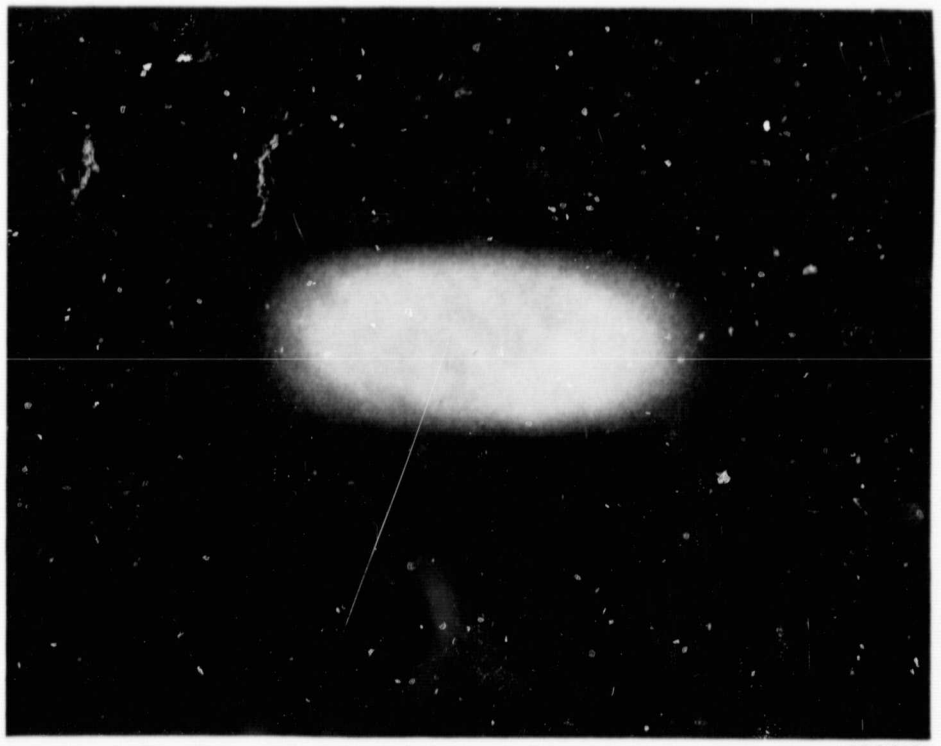

6904161

(b) At 96X Enlargement

Figure 9. Diffraction Pattern of the Target "3"

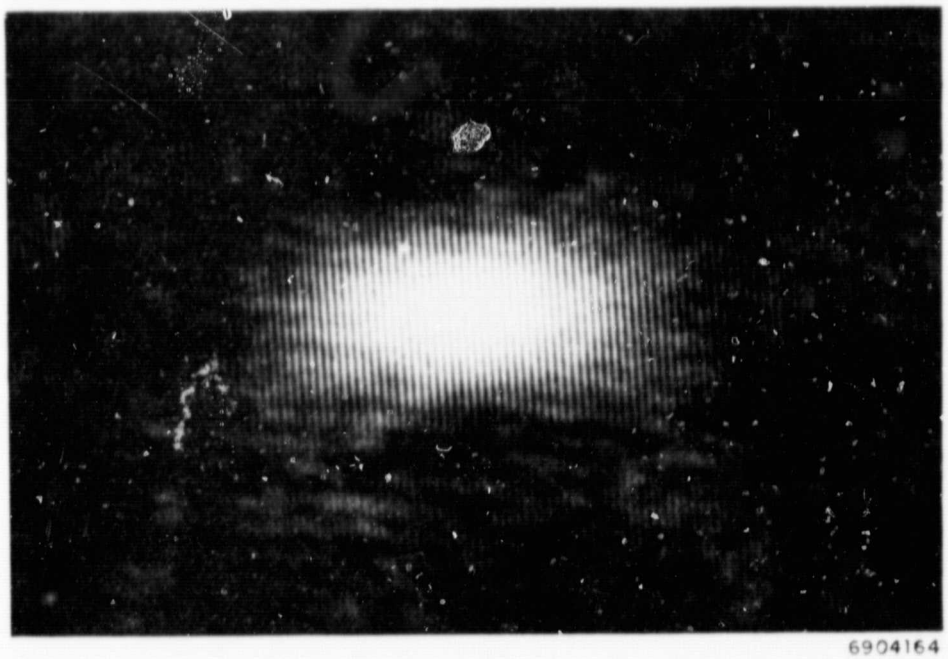

6904164

Figure 10. Hologram of the Stationary "3"

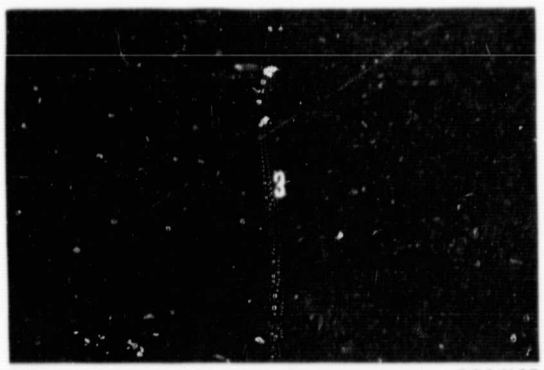

6904165

Figure 11. Reconstructed Image from the Stationary "3"

It seems as a result of these tests that the stationarity of the hologram fringes of a moving object and synchronized reference beam is sufficient. Translations of up to 2 or 3 cm could be tolerated during the exposure by selecting the best available lens.

4.2 Quality and Brightness of the Reference Beam

Experiments were carried out to estimate the irradiance from the back reflected reference beam. Polished stainless steel ball bearings were used as objects. A photomultiplier was used to measure the irradiance from the back reflected light relative to the irradiance from the collimated illumination. An unfiltered mercury arc light source was used to eliminate the coherence effects. Figure 13 is a plot from data taken with five different bearing diameters. The irradiance from the back-reflected light was measured at a distance of 40 cm from the ball bearing. The solid curve is a theoretical plot assuming the reflectivity of the bearing to be 0.2. This plot was derived from

(a) Total Translation 0.2 cm

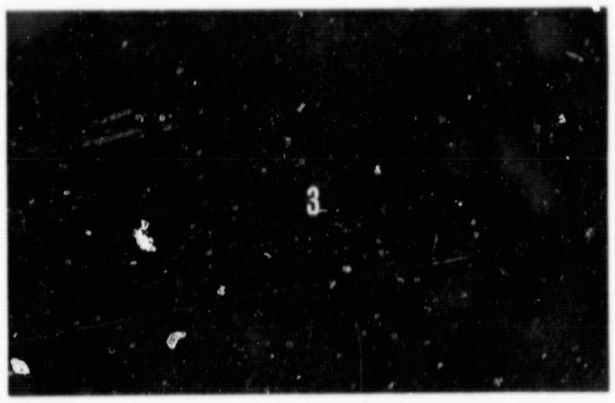

(b) Total Translation 1.2 cm

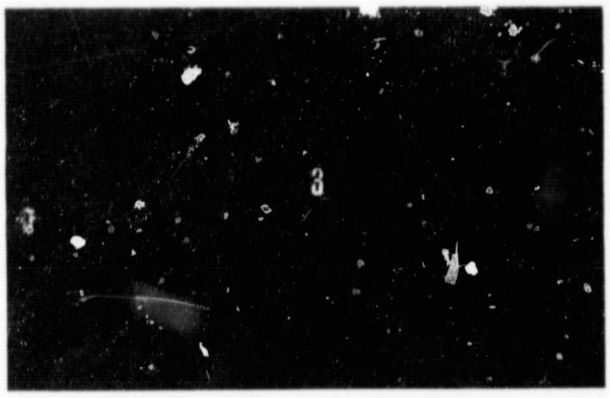

(c) Total Translation 1.8 cm

6904160

(d) Total Translation 2.4 cm

Figure 12. Reconstructions of Translated Object

geometrical optics considering the bearings to be spherical mirrors of focal length -R/2. The resulting equation is a parabola as function of the bearing radius, R,

$$\frac{E_R}{E_I} = \frac{\epsilon R^2}{4D^2} \quad . \tag{20}$$

Here, E_R and E_D are the reflected irradiance and the incident irradiance, ϵ is the bearing reflectivity, and D is the distance from the bearing to the photodetector. The data shown in Figure 13 indicate that the reflected irradiance is quite well described by Equation (20), although this derivation will not hold when the sphere approaches a few wavelengths in diameter. Table II is an estimate of the energy required for recording holograms of 50μ particles for three different films. The exposure data for the films was obtained from a previous contract and is shown in Figure 14. Here, the development was 8 minutes at 68°F in D-19.

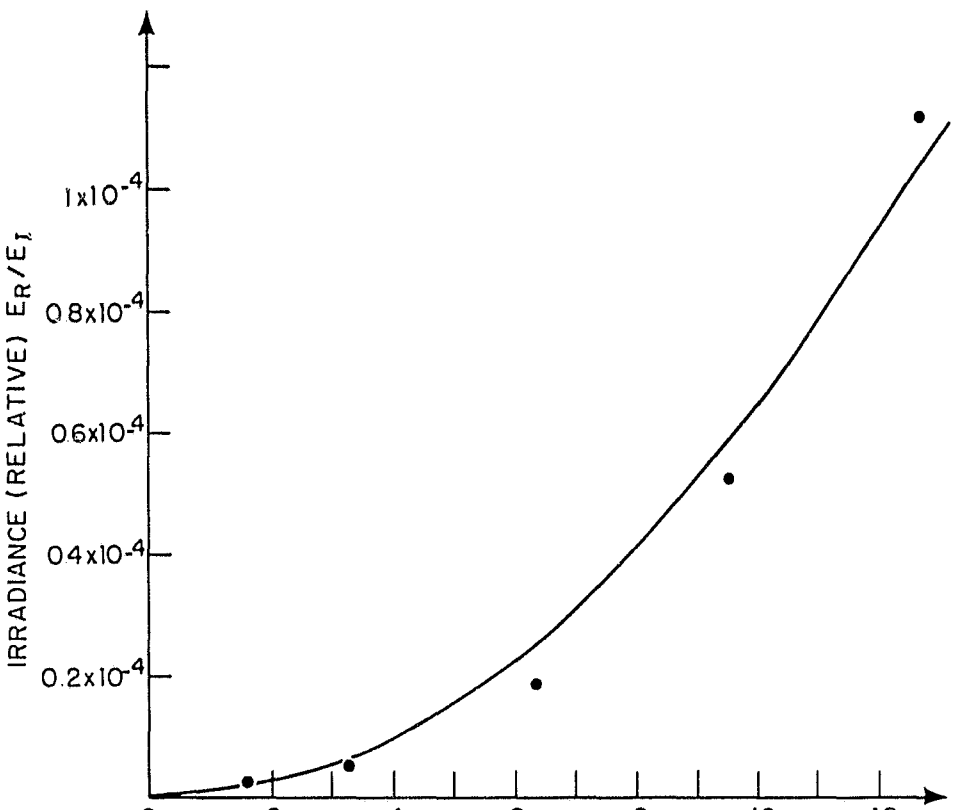

Figure 13. Plot of Back Reflected Light from Stainless Steel Balls

TABLE II
ESTIMATES OF ENERGY PER PULSE TO RECORD HOLOGRAMS OF 50μ PARTICLES

Film Type	Required Irradiance (ergs/cm^2)	Energy per Laser Pulse
8403 (Tri-X)	0.06	16 joules
SO-136 (Pan-X)	0.2	52 joules
SO-243	1	256 joules

It is assumed that the laser is collimated into a 4-sq cm beam and that a 10-cm focal length transform lens is used. It is also assumed that the optical system (collimator, interferometer, and t nsform lens) is 10 percent efficient. The estimates in Table II suggest that providing enough light would be a difficult but not insurmountable task.

An additional problem exists in the reference beam. The back-reflected light is speckled. This results because the surfaces of the polished bearings are not optically smooth. Figure 15 shows the nature of this speckling recorded at 40 cm from the bearings. Data from these and other pictures indicate that the average speckle spot size changes inversely with bearing diameter. Considering the work of other

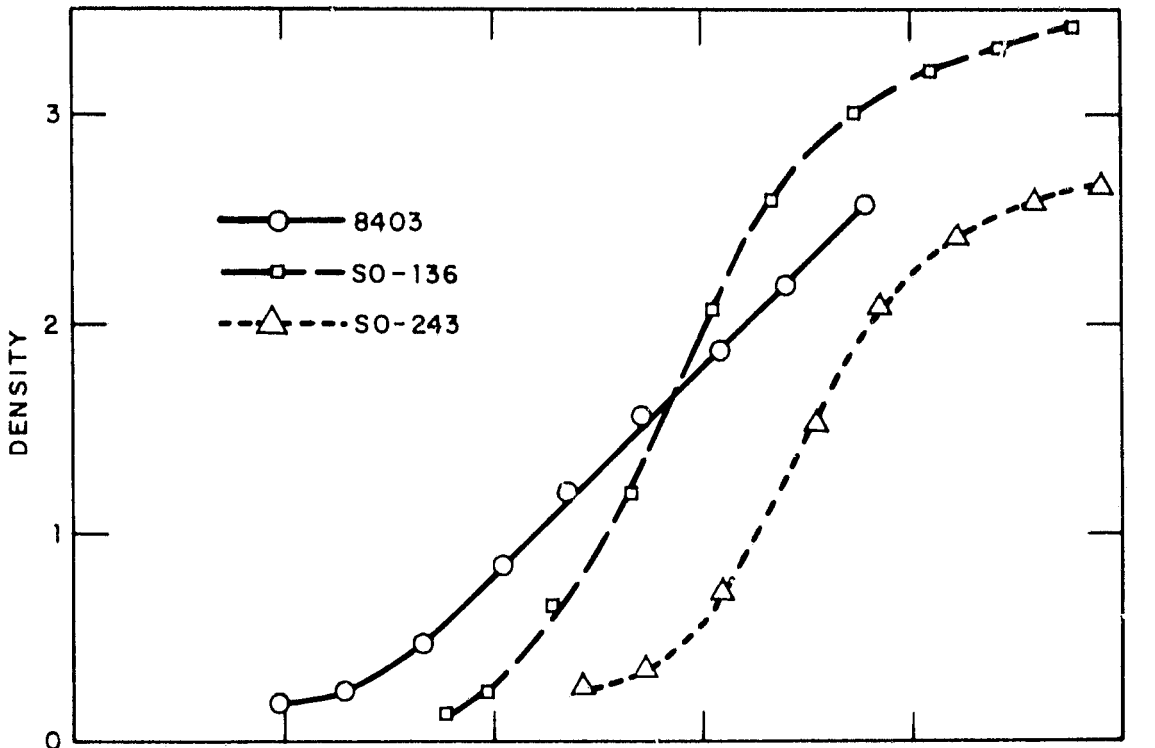

Figure 14. D vs. Log E Curves for 8403, SO-136 and SO-243 Films Exposed to Ruby Laser Illumination

researchers this effect is to be expected (Refs. 6 and 7). The important thing is the ratio of the average speckle spot size to the diameter of the forward diffraction pattern of the object. It is estimated that in the case of the ball bearings the speckle size is approximately 15 times the diameter of the fourth ring of the diffraction pattern.

To investigate the effects of speckle in the case of Fourier transform holograms, ground glass was used to create a speckled reference beam. The setup shown in Figure 7 was used except that a piece of ground glass was placed near the focus of the lens producing the point reference source. The position of the ground glass was adjusted until the average speckle spot was approximately 15 times the diameter of the fourth lobe of the diffraction pattern of the "3" target.

Five holograms were made with the randomly speckled reference beam. The ground glass was arbitrarily translated laterally to a new position for each hologram. Images (a), (c) and (e) of Figure 16 show some degradation; image (b) is of good quality; and image (d) failed to reconstruct. These data indicate that it will not be possible to predict the image quality of any given hologram. The image quality would fluctuate in random manner ranging from good images to no image at all.

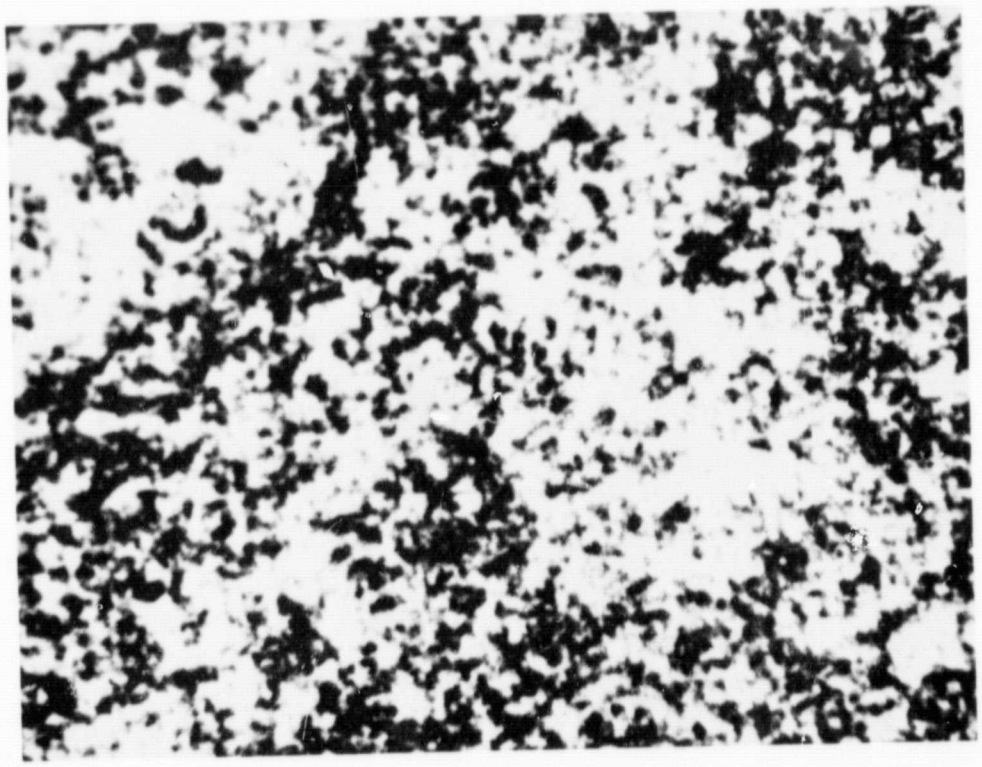

(a) 9-mm Bearing

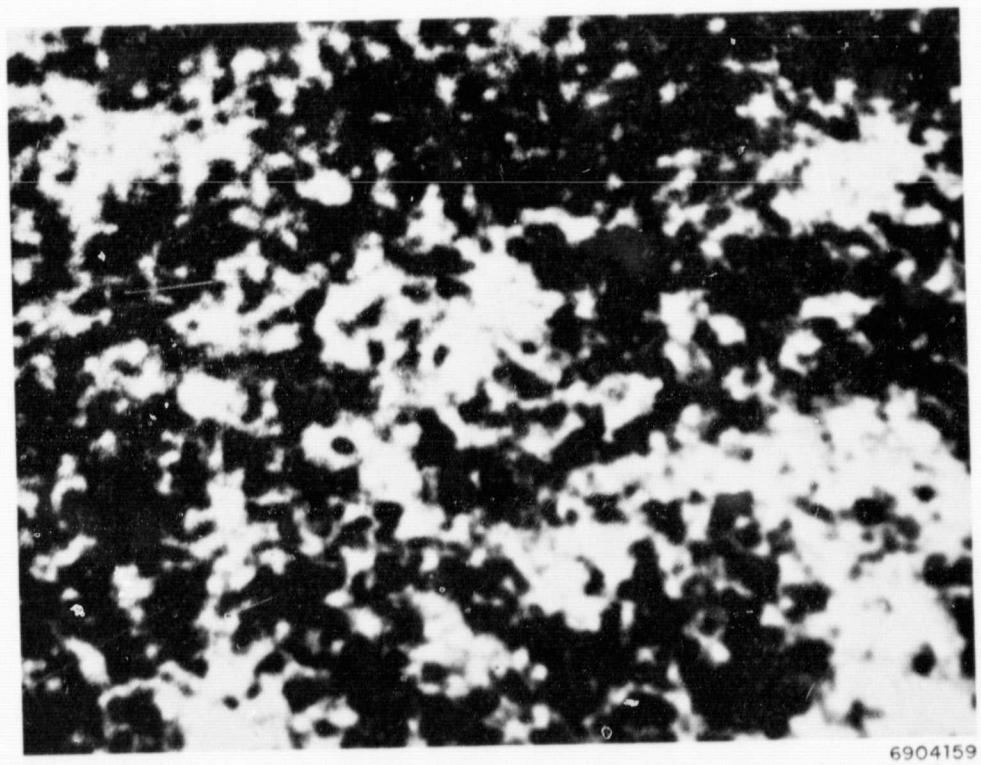

(b) 3-mm Bearing

Figure 15. Speckle Pattern from Ball Bearings

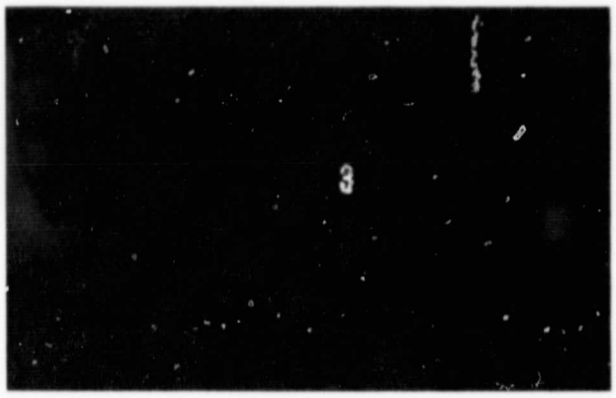

(a)

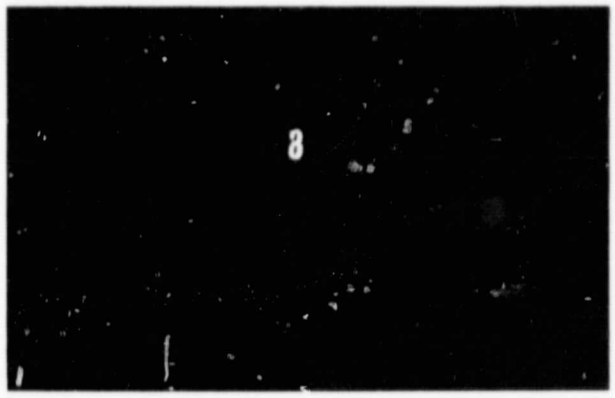

(b)

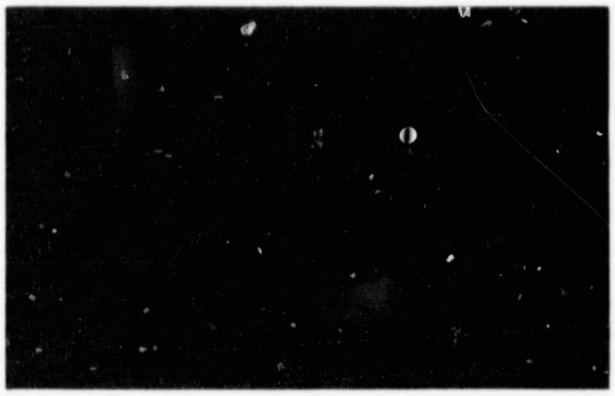

(c)

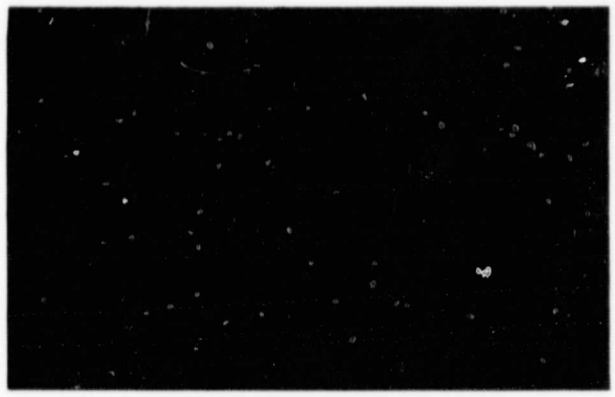

(d)

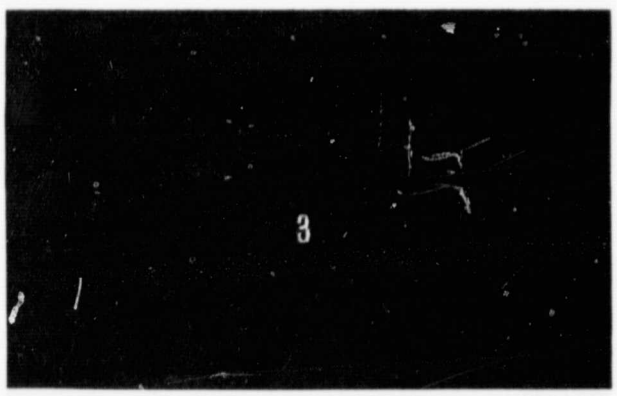

6904158

(e)

Figure 16. Reconstruction of Holograms Using a Randomly Speckled Reference Beam

4.3 Resolution of Fourier Transform Holograms

In the experiments described in the previous subsections a transparent "3" on a dark background was used as a target. Considerable resolution is lost when a dark object "3" is used as a target on a transparent background. This happens since the light in the background beam focuses at the center of the transform plane and over-exposes the film. Thus, the low frequency information is lost from the object hologram. The reconstructed image has the appearance of an image seen through a Schlieren optical system. Figure 17 shows a dark "3" on a transparent background. The "3" is the same size as the previous object.

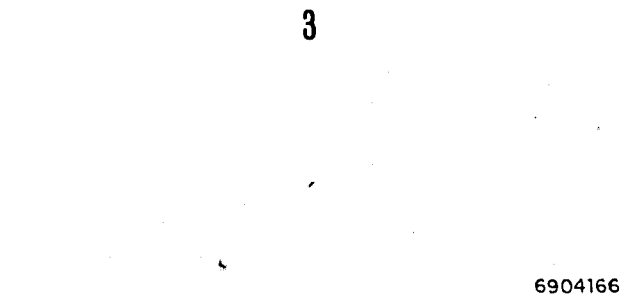

6904166

Figure 17. Target of Dark "3" on Transparent Background

Figure 18 is a Fourier transform hologram of the "3" in which the background area was stopped to be only slightly larger than the "3". The hologram was made in the setup shown in Figure 7. This hologram should be compared with the hologram in Figure 10. The strong side lobes in the hologram are caused by the rectangular background shape. Even though the light level and photographic processing were optimized to give a good reconstructed image, the interference fringes are missing in the over-exposed center spot. The reconstructed image is shown in Figure 19. Loss of the low frequencies is apparent from the dark background.

Figure 20 is the hologram of the "3" with a 1.5-cm square background. In this case lens flare greatly enlarges the size of the focused background beam. Figure 21 is the reconstructed image. Again, the edges of the beam stop are apparent along with much of the dirt and dust on the transparent area of the target. The low frequency information is now absent from the "3". To demonstrate the difficulty further, an Air Force 3-bar resolution target was hologrammed. The reconstructed image is shown in Figure 22. The resolution lies between 10 and 15 lines/mm. Although much smaller detail can be seen in the reconstruction, the lack of low frequencies adds extraneous effects to the image. These effects would be a problem if one were trying to estimate the mass of an unknown high speed particle from its hologram image. In this case too, care was taken to optimize the balance of intensity between the reference beam and object diffraction, the exposure time, and the chemical processing. Further checks were carried out to insure that the problem was not caused by the lens or the hologram film.

Two experiments were attempted to minimize the intensity of the background light at the center of the hologram. First, a dark field interferometer was set up. This was essentially a Mach-Zehnder which was adjusted to give a fringe minimum across the entire output field. When an object was placed in one arm, the diffraction pattern of the object would appear on the dark field. This proved too sensitive to be

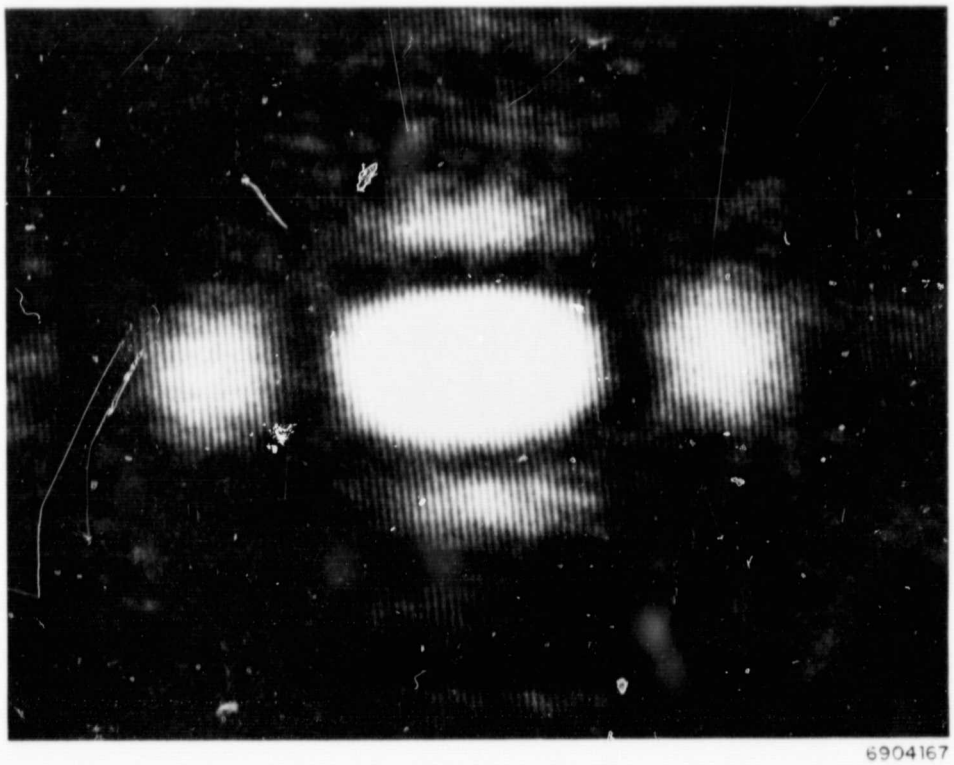

6904167

Figure 18. Hologram of Dark "3" on Small Rectangular Background

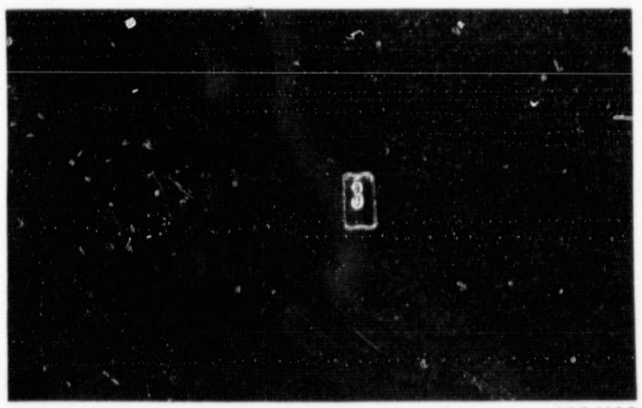

6904168

Figure 19. Reconstruction of Hologram in Figure 18. (Edges of the background aperture are apparent although the background is dark.)

implemented with a pulsed laser. A second approach using tapered circularly symmetric density masks in the transform plane was tried. Although good results were not obtained in the limited time available, this method does have some promise. Extended range processing techniques could also be tried.

4.4 The Interferometer System

The last experiment carried out was to verify the interferometer system pictured in Figure 4. The experiment was performed by placing the Mach-Zehnder interferometer part of the system in Figure 4 between the target and transform lens shown in Figure 7. The system is shown in Figure 23. Polarized light was not used. Since a point reference is produced in the target plane by the microscope lens, either arm of the interferometer could produce a Fourier transform hologram. Figure 24 is the reconstructed image from a hologram made through one arm of the interferometer. The round spot at

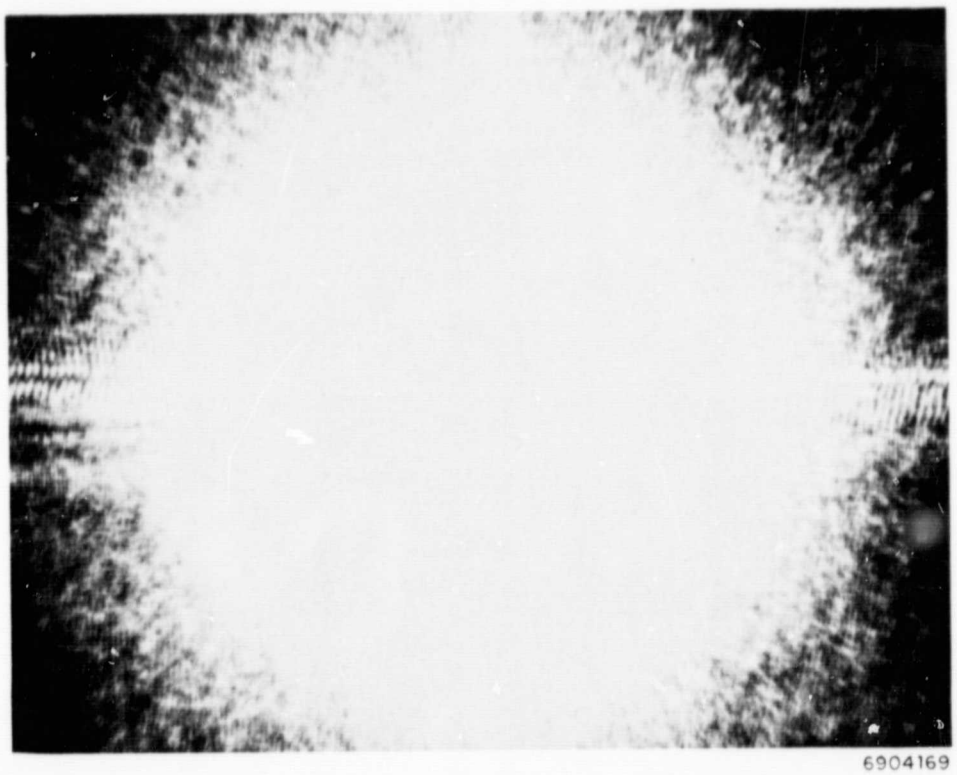

6904169

Figure 20. Hologram of "3" on 1.5-cm Square Transparent Background

6904170

Figure 21. Reconstruction from Hologram of "3" on 1.5-cm Square Background

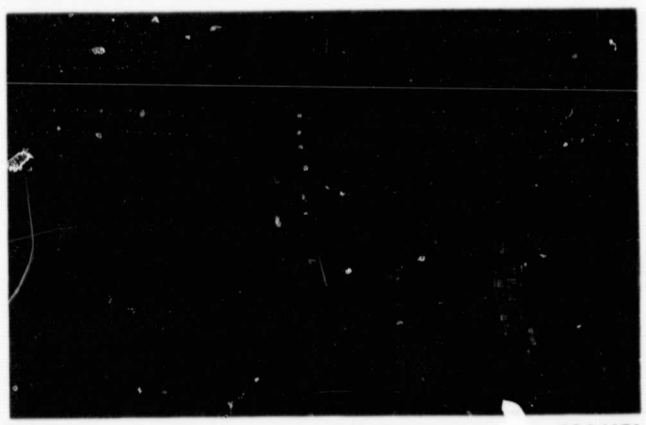

6904171

Figure 22. Reconstructed Image of an Air Force 3-Bar Resolution Target. (The original target had black bars on a transparent background. Magnification is 5X.)

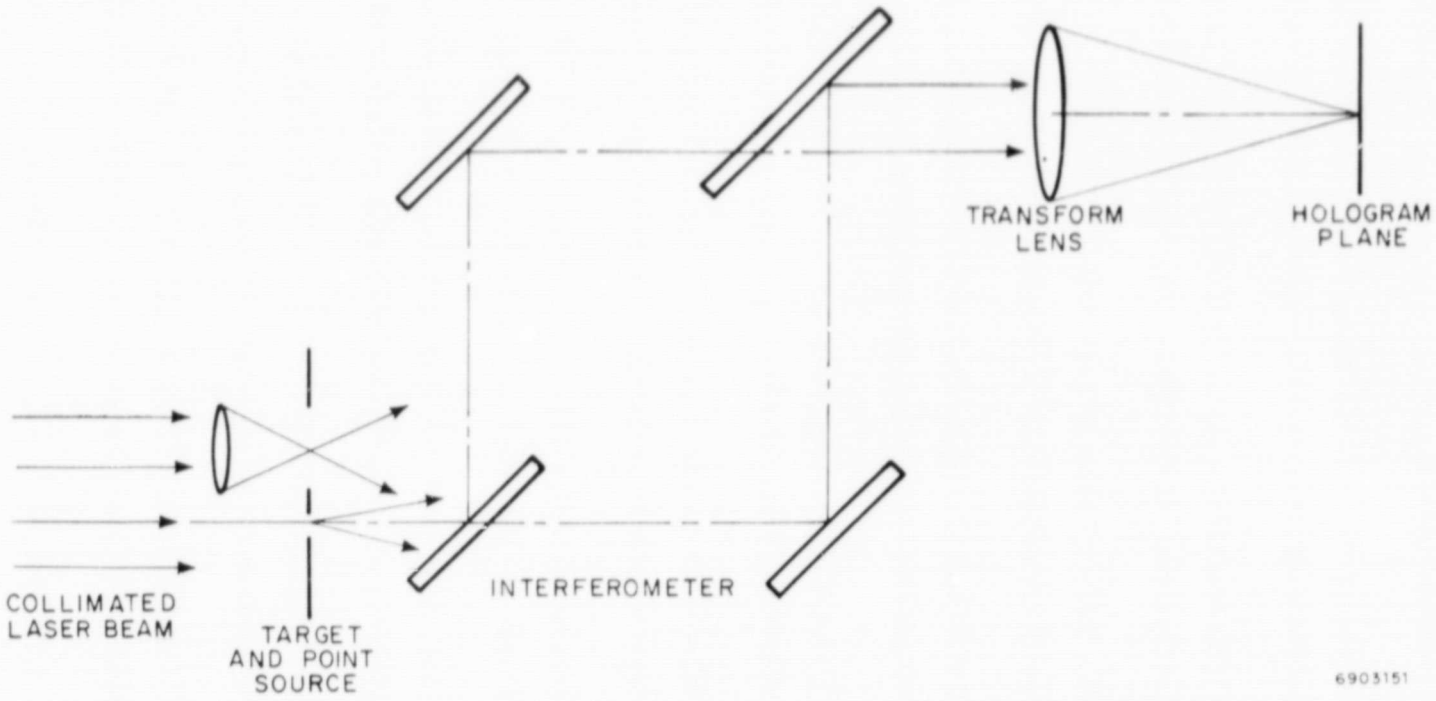

Figure 23. Experimental Setup of Interferometer System

Figure 24. Reconstruction of Hologram Recorded through One Arm of the Interferometer. (The hologram DC spot appears at the right.)

the right of the photograph is the dc order of the hologram. The square shaped object is due to multiple reflections in the beam splitters. The original target was the transparent "3" which reconstructs on the left.

A second hologram was made using both arms of the interferometer. The reference beam was blocked by an aperture in the lower arm, and the object diffracted light was blocked by an aperture in the upper arm. Thus, polarized light was not needed to separate the two beams, one in each arm. A double exposure hologram was made while the object was translated 2 mm. The reconstructed image is shown in Figure 25. The increased distance between the "3" and the dc order is due to the displacement introduced by the interferometer. This demonstrates the stationarity of the interferometer system.

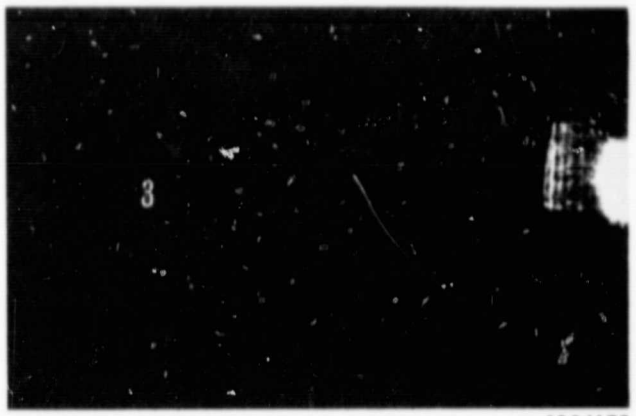

6904173

Figure 25. Reconstructed Image of Hologram Recorded through Both Arms of the Interferometer while the Object was Translated 2mm. (The increased separation between the "3" and the DC order is due to the displacement introduced by the interferometer.)

SECTION 5

CONCLUSIONS

The feasibility of recording automatically synchronized holograms of high speed particles was investigated theoretically and experimentally. An interferometer system was introduced and studied. It was shown that holograms can be recorded by this system while the object is translated during the exposure. There remain several difficulties which prevent this approach from being immediately applicable to the problem intended. At this point the worst drawback is the lack of resolution and extraneous effects in Fourier transfer holograms of small dark objects on a bright background. This difficulty is caused by the inability of the method to record in the hologram low frequency information. This is a general problem in Fourier transform holography and not particular to the motion problem. Two methods, tapered density masks and extended range development, hold promise of increasing the resolution. Time did not allow a full investigation of these methods under the current program. Two additional but less severe difficulties are the high light levels required and the speckled back-reflected beam. Based on the results of this study, it is suggested that the interferometer system for providing a synchronized reference beam would be applicable for high speed objects 100 μ and larger. Until resolution can be increased, it is not feasi-feasible to consider this approach for particles less than 100 μ diameter.

Before this system is pursued further for small particles, other approaches should be given some consideration. One such approach would be to use a mode locked ruby laser as a light source. One or more pulses can be electronically gated out. The duration of each pulse can be 10^{-10} sec or less. Pulses of this duration are short enough to stop a 10 μ particle at 10 Km/sec or a 50 μ particle at 50 Km/sec. This light source could be used with the Ronchi ruling hologram technique (Refs. 8 and 9). This method requires a minimum of spatial and temporal coherence since the object interferes with itself. Holograms may be recorded in the near field of the object or up to 100 far field distances away. Thus, depth of field would be no problem. Spatial resolution of 80 lines/mm has been obtained. This is equivalent to good resolutions of 15 μ diameter particles.

SECTION 6

REFERENCES

1. Thompson, B. J., Ward, J. H. , .nd Zinky, W. R. ; "Application of Hologram Techniques for Particle Size An sis," Applied Optics, 6, 3, March 1967.

2. Born, M., and Wolf, E. ; Principles of Optics, The MacMillan Company, 1964.

3. DeVelis, J. B., and Reynolds, G. O. ; Theory and Applications of Holography, Addison-Wesley Publishing Company, 1967.

4. Beran, M. J., and Parrent, G. B. Jr. ; Theory of Partial Coherence, Prentice-Hall, Inc., 1964.

5. Stroke, G. W. ; An Introduction to Coherent Optics and Holography, Academic Press, 1966.

6. O' Neill, E. L. ; Introduction to Statistical Optics, Addison-Wesley, 1963.

7. Ward, J. H. ; "Scattering of Laser Radiation by a Time-Varying Random Scatterer," JOSA 58, 5, p. 715, May 1968.

8. Ward, J. H., and Dyes W. A. ; "Feasibility Study for Airborne Ice-Crystal Disdrometer," Final Report AFCRL-68-0519, Contract No. F19628-67-C-0140, September 1968.

9. Dyes, W. A., and Ward, J. H. ; "Versatile Two-Beam Hologram System," JOSA 58, 5, p. 723, May 1968.

NEW TECHNOLOGY APPENDIX

AUTOMATIC REFERENCE BEAM SYNCHRONIZATION FOR FOURIER TRANSFORM HOLOGRAMS

A method for deriving an automatically synchronized reference beam for Fourier transform holograms of moving objects is described on pages 8 through 12 and on pages 23 and 25 of this report. This technique would be applicable for hologramming hypervelocity particles of greater than 100 μ diameter.